

## Increased antiprotease activity of the SERPINB3 polymorphic variant SCCA-PD

Cristian Turato<sup>1</sup>, Alessandra Biasiolo<sup>2</sup>, Paolo Pengo<sup>3</sup>, Vladimir Frecer<sup>4,5</sup>, Santina Quarta<sup>2</sup>, Silvano Fasolato<sup>2</sup>, Mariagrazia Ruvoletto<sup>2</sup>, Luca Beneduce<sup>3</sup>, Jessica Zuin<sup>3</sup>, Giorgio Fassina<sup>3</sup>, Angelo Gatta<sup>2</sup> and Patrizia Pontisso<sup>2</sup>

<sup>1</sup>Istituto Oncologico Veneto IOV-IRCCS, Via Gattamelata, 64-35128 Padova; <sup>2</sup>Department of Clinical and Experimental Medicine, University of Padua, Via Giustiniani, 2-35128 Padova; <sup>3</sup>Xeptagen SpA, VEGA Science Park, Via delle Industrie, 9-30175 Marghera (VE), Italy; <sup>4</sup>Department of Physical Chemistry of Drugs, Faculty of Pharmacy, Comenius University, Odbojarov 10, 83232 Bratislava; <sup>5</sup>Cancer Research Institute, Slovak Academy of Sciences, Dúbravská cesta, SK-8339 Bratislava, Slovakia  
Corresponding author: Professor Patrizia Pontisso, Clinica Medica 5 – Department of Clinical and Experimental Medicine, Via Giustiniani, 2-35128 Padova, Italy. Email: patrizia@unipd.it

### Abstract

SERPINB3 has been found in chronic liver damage and hepatocellular carcinoma, but not in normal liver. By direct mRNA sequencing, a new SERPINB3 polymorphism (SCCA-PD) has been identified, presenting the substitution Gly351Ala in the reactive center loop of the protein. The prevalence of the SCCA-PD isoform has been found to be significantly higher in patients with cirrhosis than in patients with chronic liver disease and in normal subjects. The aim of this study was to investigate the biological and functional activity of SERPINB3 isoforms using *in vitro* models. HepG2 and Huh7 cells lines were transfected with plasmid vectors containing wild-type SERPINB3 or its polymorphic variant SCCA-PD and their expression at transcriptional and protein level was determined. To assess the functional activity, both recombinant proteins were produced and kinetic analysis was carried out using papain and cathepsin-L as target proteases. In addition, the inhibition of JNK kinase activity by SERPINB3 isoforms was assessed. The crystal structure of wild-type SERPINB3 at 2.7 Å resolution was used for preparation of refined 3D models of the two isoforms. The results showed that transcriptional activity and protein expression of the two isoforms were similar in both transfected cell lines. Both SERPINB3 preparations exerted a dose-dependent protease inhibitory activity, but the effect of SCCA-PD was higher than that of the wild-type isoform. This result was supported by 3D modelling, where increased hydrophobic profile of the SCCA-PD isoform, introduced by the G351A mutation, was detected. In addition, at high protein concentration, SCCA-PD revealed a 16% higher inhibitory effect on c-Jun phosphorylation by JNK1, compared with wild-type SERPINB3. In conclusion, the single amino acid substitution in the SERPINB3 reactive site loop improves the functional activity of SCCA-PD isoform. This different antiprotease activity might favor disease progression in patients carrying this polymorphism.

**Keywords:** clade B serpins, single nucleotide polymorphism, enzymatic activity

*Experimental Biology and Medicine* 2011; **236**: 281–290. DOI: 10.1258/ebm.2011.010229

### Introduction

SERPINB3, formerly known as Squamous Cell Carcinoma Antigen-1 or SCCA-1, is a member of the ovalbumin family of serine proteinase inhibitors.

The protein was initially isolated from a metastatic cervical squamous cell carcinoma by Kato and Torigoe.<sup>1</sup> SERPINB3 is detected in the superficial and intermediate layers of normal squamous epithelium, while its mRNA is detectable in the basal and sub-basal levels. This serpin has been used in the clinical setting as a circulating tumor

marker for squamous cell tumors, especially those of the cervix, head and neck, lung and esophagus.<sup>2</sup>

SERPINB3 has been also detected in damaged liver tissue and high amounts have been observed at the transcription and protein levels in neoplastic and highly dysplastic cells but not in normal liver.<sup>3–5</sup> By direct mRNA sequencing, a new SERPINB3 polymorphic variant (SCCA-PD) has been identified in cases of hepatocellular carcinoma, presenting the 351<sub>G→A</sub> mutation in the reactive site loop (RSL) of the protein<sup>3</sup> (GeneBank accession number: EU852041, SNP

identification rs3180227). Since the mechanism of protease inhibition by serpins involves a profound change in conformation, initiated by interaction of the protease with the reactive center of the serpin, the specific amino acid change detected in the reactive center of SCCA-PD might confer a different biological behavior to the serpin.

Inhibitory serpins function via an exposed RSL of about 20 amino acids and irreversibly inhibit proteinases through a suicide substrate inhibition mechanism. The enzyme recognizes and binds the RSL, forming a serpin-enzyme complex (SEC).<sup>6</sup> This leads to cleavage of the RSL between the reactive P1 and P1' residues, causing a significant and irreversible conformational change with complete insertion of the RSL loop into a  $\beta$ -sheet. The enzyme is inactivated by the formation of an acyl ester linkage between the active serine site and a serpin side chain.<sup>7,8</sup> Although in these conditions the SEC is kinetically stable, it is thermodynamically unstable and could eventually break down, releasing inactivated (cleaved) serpin and active proteinase. Therefore, the irreversible inhibition of the proteinase requires removal of the SEC from the circulation.<sup>7</sup>

The reactive site of a serpin consists of a loop projecting from the body of the protein, comprising a hinge region and a variable reactive center loop. Site-directed mutagenesis has been used to examine the role of individual residues within the RSL.<sup>8-11</sup> Previous studies of inhibition of serine proteinase by serpins demonstrate that alteration to the hinge region affects serpin activity by altering the RSL mobility and the rate at which the RSL inserts into the serpin. Mutation of the P14 residue from alanine to arginine blocks RSL insertion and abrogates inhibitory activity, although the protein still functions as a substrate.<sup>9</sup> Mutation of the variable region has shown that the P3 residue is critical in the interaction between cathepsin-S and SERPINB3, such that mutation of the P3 phenylalanine to alanine results in a loss of cathepsin-S inhibition.<sup>9</sup>

The effect of SCCA-PD variant, presenting the Gly351Ala mutation, in the reactive center of the protein (P4) has not yet been studied.

The aim of the present study was to investigate the biological behavior and functional activity of the new SERPINB3 mutant, compared with wild-type, using *in vitro* models of transient cell line transfection and recombinant SERPINB3 proteins.

## Materials and methods

### Construction of SERPINB3 expression vectors

SERPINB3 cDNA was obtained from total RNA extracted from surgical liver biopsies of hepatocellular carcinoma of patients carrying the two different SERPINB3 variants: SERPINB3 wild type (accession number NM\_006919) and

SCCA-PD (Gly351Ala; accession number EU852041). Total cellular RNA was extracted using the Trizol reagent (Invitrogen, Carlsbad, CA, USA). First strand cDNA was synthesized (Superscript II reverse transcriptase, Invitrogen) and subsequently amplified by nested polymerase chain reaction (PCR), using two pairs of specific oligonucleotide primers (Invitrogen), described in Table 1, and Pwo DNA Polymerase (Roche Diagnostics GmbH, Indianapolis, IN, USA). PCR cycling for both reactions was performed in the Thermal Cycler 480 (Perkin Elmer, Norwalk, CT, USA) as follows: 94°C for three minutes, followed by 55°C for 60 s, and 72°C for 60 s (1 cycle); 94°C for 60 s, followed by 55°C for 60 s, and 72°C for 60 s (32 cycles) and the last cycle of 94°C for 60 s, followed by 55°C for 60 s, and a final extension step (72°C for 3 min).

The obtained PCR fragment was cloned directly into the mammalian expression vector pcDNA3.1D/V5-His-TOPO (Invitrogen). The construct was propagated into *Escherichia coli* TOP10 competent cells (Invitrogen) and purified using the Genopure Plasmid Maxi kit (Roche Applied Science, Indianapolis, IN, USA).

The expression constructs were verified by restriction digestion and DNA sequencing using an ABI 310 automated DNA sequencer (Applied Biosystems, Foster City, CA, USA), according to the manufacturer's instructions. The alignment analysis (using nucleotide BLAST) confirmed complete sequence homology of the SERPINB3 inserts with the published sequences of the two mRNA SERPINB3 isoforms (NM\_006919 and EU852041). pcDNA3.1, lacking the SERPINB3 insert, was used as a negative control.

### Cell lines transfection

HepG2 and Huh7 cell lines were transiently transfected with plasmid vectors carrying SERPINB3 and SCCA-PD, constructed as described above, or with the empty vector, as control. Cells were plated in six-well plates at a density of  $1 \times 10^6$  and  $8 \times 10^5$  cells/well (~60% confluence), respectively, 24 h before transfection. Cells were then incubated with 1  $\mu$ g of plasmid DNA/well in the presence of Lipofectamin Reagent and Plus Reagent (Invitrogen). After five hours incubation at 37°C in a humidified atmosphere containing 5% CO<sub>2</sub>, wells were washed twice with OptiMEM (Invitrogen) and incubated with fresh RPMI medium (Sigma-Aldrich, St Louis, MO, USA) supplemented with 10% fetal bovine serum for further 120 h.

### Characterization of SERPINB3 expression

#### Quantitative realtime reverse transcription-PCR

The levels of SERPINB3 mRNA in transfected cells were measured with the realtime reverse transcription (RT)-PCR

**Table 1** Primer pairs used for construction of SERPINB3 expression vectors

Primers pair set	Sequence 5'–3'	Position (mRNA)
primer-1 out For	CACAGGAGTTCAGATCACATCGAG	–31/–7
primer-2 out Rev	CTGGAAGAAAAAGTACATTATATGTGGGC	+1355/+1384
primer-3 in For	CACCATGAATTCAGTCAAGCCA	–1/+21
primer-4 in Rev	ATTGCATCTACGGGGATGAG	+1161/+1181

For, forward; Rev, reverse

method using SYBR® green. Total RNA was purified from cells grown in monolayer with the Trizol reagent (Invitrogen), following the manufacturer's instructions. RT-PCR was performed with 2  $\mu$ L of cDNA, synthesized after standard reverse transcription of extracted RNA. The amplification mix was prepared using Roche LightCycler FastStart DNA Master<sup>PLUS</sup> SYBR Green I kit, following the manufacturer's instructions, and realtime PCR was performed using the LightCycler instrument (Roche Diagnostics GmbH). The oligonucleotide sequences of primers designed for realtime PCR were the following: SERPINB3 sense 5'-GCA AAT GCT CCA GAA GAA AG-3', SERPINB3 reverse 5'-CGA GGC AAA ATG AAA AGA TG-3'; housekeeping gene: GAPDH sense 5'-TGG TAT TCG GGA AGG ACT CAT GAC-3', GAPDH reverse 5'-ATG CCA GTG AGC TTC CCG TTC AGC-3'.

The single-tube RT-PCR assay for SERPINB3 was performed on the LightCycler and consisted of one denaturation cycle at 95°C for 10 min, 45 cycles of amplification at 94°C for one second, 62°C for 10 s and 72°C for 10 s followed by a melt from 72 to 98°C rising at 0.1°C/s. The capillaries were then cooled to 37°C for 30 s. The fluorescence of the SYBR green dye was determined as a function of the PCR cycle number, giving the threshold cycle ( $C_T$ ) number. The  $C_T$  values were used to quantify the PCR product;  $\Delta C_T$  was calculated by subtracting  $C_T$  (control gene: GAPDH) from  $C_T$  (target gene: SERPINB3). The  $\Delta C_T$  value of a control (untransfected cells) was arbitrarily used as a constant that was subtracted from all other  $\Delta C_T$  values to determine  $\Delta\Delta C_T$  value. Samples were run in triplicate and fold changes were then generated for each sample by calculating  $2^{-\Delta\Delta C_T}$ .

### Fluorescence techniques

The expression of SERPINB3 in transiently transfected and control HepG2 and Huh7 cells was assessed by immunofluorescence. Cells were seeded on slides ( $2 \times 10^5$  HepG2 cells/slide) and cultured for 48 h. Cells were fixed in 4% paraformaldehyde, permeabilized in 0.2% Tryton X100 and blocked with 5% bovine serum albumin in phosphate-buffered saline (PBS). Slides were then incubated at room temperature for two hours with 10  $\mu$ g/mL of a monoclonal anti-SCCA antibody (Xeptagen, SpA, Marghera, VE, Italy), washed with 0.1% Tween 20 in PBS and incubated with the TRITC-conjugated secondary antibody (1:50 dilution) (Dako, Copenhagen, Denmark) at room temperature for two hours. The cellular nuclei were stained by cell incubation with 20  $\mu$ g/mL of Hoechst 33342 (Sigma-Aldrich) for five minutes. Slides were washed in PBS, mounted with glycerol (Sigma-Aldrich) and observed under confocal microscope ViCo (Nikon, New York, NY, USA).

### Enzyme-linked immunosorbent assay

To assess the amount of recombinant SERPINB3 protein isoform produced in transfected cells, their concentration was measured in parallel in the supernatant and in cellular extracts of transfected cells using an enzyme-linked immunosorbent assay (ELISA) kit (Xeptagen), following the manufacturer's instructions. Sample concentration of

recombinant SERPINB3 protein was calculated on the basis of a standard curve included in the ELISA kit.

### Expression and purification of recombinant SERPINB3 proteins

SERPINB3 wild-type cDNA and SCCA-PD cDNA were cloned in the directional expression vector pET101 (Invitrogen).

The resultant blunt-ended SERPINB3 cDNA, complementary to -1/ + 21 and +1161/ + 1181 regions of SERPINB3 mRNA, was ligated with the pET101 directional TOPO vector (1 and 1  $\mu$ L salt solution; Invitrogen) for 15 min at room temperature. A volume of 50  $\mu$ L of top 10 chemically competent *E. coli* (Invitrogen) were transformed by incubation with 3  $\mu$ L of ligation mix for 30 min on ice, followed by a heat shock of 42°C for 30 s. SOC medium (250  $\mu$ L; Invitrogen) was added to the cells and they were then incubated at 37°C for 30 min in a shaking bath. The transformation mix (100  $\mu$ L) was then plated on a LuriaBertoni (LB) plate (100  $\mu$ g mL<sup>-1</sup>) and incubated overnight at 37°C. The sequence of the insert of the constructed plasmid pET101/SERPINB3 was verified as described above.

The purified plasmids (40 ng each) were transformed into BL21 Star (DE3) cells (Invitrogen) for SERPINB3 expression. After SOC addition and incubation, the culture was transferred to fresh LB (10 mL) and grown overnight at 37°C in a shaking bath. 1 mL of the culture was then transferred into 100 mL of fresh LB and was grown at 37°C under shaking. For the production of SERPINB3 proteins, isopropylthio- $\beta$ -galactoside (isopropyl-beta-thio galactopyranoside, 1 mmol L<sup>-1</sup> final concentration; Roche Diagnostics GmbH) was added when the culture had attained an optical density of 0.6 at a 600 nm wavelength, and the culture was incubated at 30°C and 200 revs/min.

Preliminary experiments were carried out to optimize the rates of SERPINB3 protein production. The maximal amount of recombinant protein production was reached four hours after induction.

The bacteria were recovered by centrifugation and washed three times with PBS buffer. The recovered pellet was resuspended in PBS (4 mL/300 mg, wet weight) and sonicated with the Ultrasonic W-380, using the immersion probe microtip 419A, f 4.8 mm (Heat Systems Ultrasonics, Farmingdale, NY, USA). The sonication was stopped at 95–98% of lysis of the bacteria, as checked with an optical microscope. The crude bacterial extract was centrifuged at 15,000g, at 4°C for 30 min to separate the soluble and the insoluble fractions. The soluble fraction was dialyzed against 20 mmol/L 2-(N-morpholino)ethanesulfonic acid (MES), pH 6 (buffer A), and the protein concentration was determined with the Bio-Rad Protein Assay kit. The dialyzed soluble fraction was diluted in buffer A to reach a final concentration of 500  $\mu$ g/mL. A glass column (25  $\times$  0.5-cm inner diameter) (Omnifit, Diba Industries, Cambridge, UK) was filled with cationic exchange Source 30S resin (Amersham Pharmacia Biotech, Uppsala, Sweden) and equilibrated at a flow rate of 3.0 mL/min with buffer A. The diluted soluble fraction was then loaded on the column, and following the elution of



unretained material, a gradient from 0% to 100% of buffer B (20 mmol/L MES, pH 6.0, 0.5mol/L NaCl) was applied to elute bound proteins. The retained fraction was recovered and dialyzed against PBS, pH 7.5.<sup>12</sup>

Recombinant SERPINB3 proteins were characterized by SDS-polyacrylamide gel electrophoresis with Coomassie blue staining.

### Kinetic analysis

The inhibitory activity of SERPINB3 isoforms against cysteine proteinases was assessed by monitoring their effect on papain (Sigma-Aldrich, Fluka) and cathepsin-L (Sigma-Aldrich) catalyzed hydrolysis of rhodamine110 bis-(Z-L-phenylalanyl-L-arginyl)amide, (Z-FR)<sub>2</sub>R110, taken as substrate. The commercially available dihydrochloride salt of the substrate (Molecular Probes, Invitrogen) was used through the study. The kinetics measurements were performed in a microtiter plate format using OptiPlate plates (Perkin Elmer); the release of the fluorescent product was monitored recording the fluorescence emission at 521 nm using an excitation wavelength of 499 nm. All the kinetic measurements were run at 25°C using a Victor X3 multilabel plate reader (Perkin Elmer) controlled by the WorkOut 2.5 software (Perkin Elmer). The raw fluorescence data were expressed as relative fluorescence units (rfu). The reactions were carried out in 50 mmol/L sodium acetate buffer pH 5.5 containing 4 mmol/L dithiothreitol and 1 mmol/L EDTA, hereinafter referred to as reaction buffer.

### Active site titration of papain and cathepsin-L

The exact concentration of active enzyme was determined by active site titration, performed according to a modified Barrett method.<sup>13</sup> A fixed amount of enzyme solution, obtained diluting a concentrated stock with reaction buffer, was incubated for one hour at room temperature with increasing concentrations of the irreversible cysteine-proteinase inhibitor E64, *trans*-Epoxysuccinyl-L-leucylamido(4-guanidino)butane (Sigma-Aldrich). The residual enzymatic activity was assayed by adding an excess (Z-FR)<sub>2</sub>R110. The substrate final concentration to test cathepsin residual activity was set to 0.5 μmol/L, while in the case of papain the concentration was set to 0.1 μmol/L. The release of the fluorescent product was monitored over time. The residual enzyme activity after incubation with each different concentration of E64 was expressed as the ratio of the initial rates measured in the presence of E64 and that measured in a control experiment in the absence of inhibitor. For the two considered enzymes, the concentrations of E64 spanned the range 0–1250 nmol/L.

### Kinetics of the interaction between SERPINB3 isoforms and the cysteine proteinases papain and cathepsin-L

The kinetic analysis of the interaction between SERPINB3 wild-type and SCCA-PD with the cysteine proteinases papain and cathepsin-L was performed under first-order conditions using the progress curve method.<sup>14,15</sup> Inhibition experiments were performed using different amounts of SERPINB3 isoforms for papain (range 0–100 nmol/L) and

for cathepsin-L (range 0–50 nmol/L). Each enzyme (1.50 and 1.68 nmol/L) was mixed with increasing amounts of inhibitors in the presence of an excess substrate (250 nmol/L for cathepsin and 500 nmol/L for papain) and the formation of the fluorescent product was monitored over time. The release of the fluorescent product was fitted to the following model:  $P = v_s t + (v_z - v_s)(1 - e^{-k_{\text{obs}} t})/k_{\text{obs}}$ ,<sup>14</sup> where a zeroth order and a simple exponential decay with observed rate constant  $k_{\text{obs}}$  were considered. In the case of cathepsin, the zeroth-order contribution was disregarded since in the fitting process  $v_s$  vanished and the overall curve was better described by the model  $P = v_z(1 - e^{-k_{\text{obs}} t})/k_{\text{obs}}$ .<sup>15</sup> The  $k_{\text{obs}}$  obtained at different concentrations of the inhibitors were plotted against the inhibitor concentration; the slope of these curves,  $k'$ , represented the uncorrected second-order rate constant for the association between the inhibitors and the enzyme. The proper second-order rate constant was obtained correcting these data for the substrate concentration and the appropriate  $K_m$  values, according to the equation  $k_a = k' (1 + [S]_0/K_m)$ .

### Assay of the JNK1 kinase activity

To investigate the JNK1 inhibition activity of wild-type SERPINB3 and SCCA-PD proteins, the SAPK/JNK kinase assay kit (Cell Signaling Technology, Beverly, MA, USA) and active JNK1 (Vinci-Biochem, Vinci [Firenze], Italy) were used. A variable amount of recombinant SERPINB3 isoforms (50, 100, 200 ng) was incubated with 10 ng of active JNK1 in a kinase buffer for 3 h at 4°C. Then, c-Jun beads were added and incubated overnight at 4°C. The mixture was further incubated for 30 min at 30°C and probed with an anti-phospho-c-Jun antibody using the JNK/SAPK kinase assay kit, following the manufacturer's instructions (Cell Signaling Technology).

### Molecular modelling and molecular dynamics simulations

The crystal structure of wild-type human SERPINB3 at 2.7 Å resolution (PDB entry code 2ZV6, chain B with visible RSL)<sup>16</sup> was used for the preparation of refined 3D models of wild-type SERPINB3 and SCCA-PD. The G351A residue replacement in SCCA-PD was done by the Biopolymer module of Insight-II.<sup>17</sup> Both SERPINB3 isoforms were then carefully refined by molecular mechanics energy minimization using all-atom representation, a CFF91 force field<sup>18</sup> and Discover molecular simulation software.<sup>17</sup> Non-bonding interaction distance cut-off set to 15 Å was employed and dielectric constant of 4 was used to take into account dielectric shielding effects in proteins. Minimization of the protein was carried out by relaxing the structure gradually, starting with hydrogen atoms, then proceeding with residue side chains and concluding the relaxation with freeing of all atoms including the protein backbone. In the geometry optimization, a sufficient number of conjugate gradient iterative cycles, with a convergence criterion set to average gradient of 0.01 kcal/mol<sup>-1</sup>/Å<sup>-1</sup>, was used.

Molecular dynamics (MD) was used for sampling the conformational space of the RSL, especially the backbone

conformation of the mutated residue 351, in both SERPINB3 isoforms. MD simulations were carried out for the RSL of the two isoforms; residues other than those of the RSL were kept fixed at their initial crystal structure configuration. The system was equilibrated in NVT ensemble at 300 K for over 100 ps, setting the integration time step to 1 fs and recording the trajectory every 0.1 ps, with a non-bonded interaction cut-off distance of 15 Å. MD simulation trajectories of the solvated isoforms, obtained during the last 100 ps of the data collection of the 200 ps trajectory, were used for the calculation of the local backbone conformation of the mutated residue 351.

## Results

### SERPINB3 transcriptional activity

Total RNA was purified from Huh7 and HepG2 cells transfected with both the plasmid vectors pcDNA3.1/SERPINB3 wild-type and pcDNA3.1/SCCA-PD and from the corresponding control cells transfected with the pcDNA3.1 vector alone. SERPINB3 mRNA transcripts were then assessed in each sample by realtime RT-PCR using primers specific for the human SERPINB3 gene. The analysis of SERPINB3 expression over time showed in both cell lines a progressive increase, reaching the maximal value at 72 h, while SERPINB3 transcription significantly decreased after 120 h. SERPINB3 transcription levels were similar in cells transfected with pcDNA3.1/SERPINB3 wild-type and in those transfected with pcDNA3.1/SCCA-PD ( $P > 0.005$ ), as shown in the example reported in Figure 1.

### SERPINB3 localization

SERPINB3 protein in transfected cells was revealed by immunofluorescence. As shown in Figure 2, a diffuse, granular cytoplasmic and nuclear SERPINB3 localization was detected in both Huh7 and HepG2, where high protein levels were detected. The fluorescence signals and the pattern of expression were comparable in cells expressing

SERPINB3 wild type and SCCA-PD isoforms. No SERPINB3 protein could be detected in cells transfected with the empty vector alone.

### Determination of SERPINB3 protein secretion

Recombinant SERPINB3 concentration was measured 48 h after cell transfection in the supernatant and in cellular extracts by ELISA. The recombinant protein was detected mainly in cellular extracts, while the corresponding supernatants contained 14.4% and 15.6% of the respective cellular content.

### Antiprotease activity of recombinant SERPINB3 proteins

Wild-type SERPINB3 and SCCA-PD recombinant proteins were purified by ionic exchange chromatography and characterized by sodium dodecyl sulfate polyacrylamide gel electrophoresis analysis with Coomassie blue staining. As shown in Figure 3, a main sharp band was detected migrating at the expected molecular weight (45 kDa) of SERPINB3.

In order to compare the antiprotease activity of the SERPINB3 isoforms, we examined the inhibitory effects of these two proteins on papain and cathepsin-L. We confirmed that both SERPINB3 preparations exerted a dose-dependent inhibitory activity on both target proteases. Using (Z-FR)<sub>2</sub>R110 as substrate, preliminary experiments provided a  $K_m$  of  $650 \pm 110$  nmol/L for papain and  $27 \pm 3$  nmol/L for cathepsin-L. In the example of Figure 4, using papain, the inhibitory activity of SCCA-PD (Figure 4a) was stronger than the activity of SERPINB3 wild-type (Figure 4b) at all considered concentrations.

The calculated second-order association constant using papain was  $(6.3 \pm 2.1) \times 10^4$  mol/L<sup>-1</sup>s<sup>-1</sup> for SERPINB3 wild-type and  $(4.1 \pm 0.7) \times 10^5$  mol/L<sup>-1</sup>s<sup>-1</sup> for SCCA-PD, accounting for a 6.5 times faster association for the SCCA-PD isoform (Figure 5a). A similar behavior was observed with cathepsin-L, although in this case a smaller difference

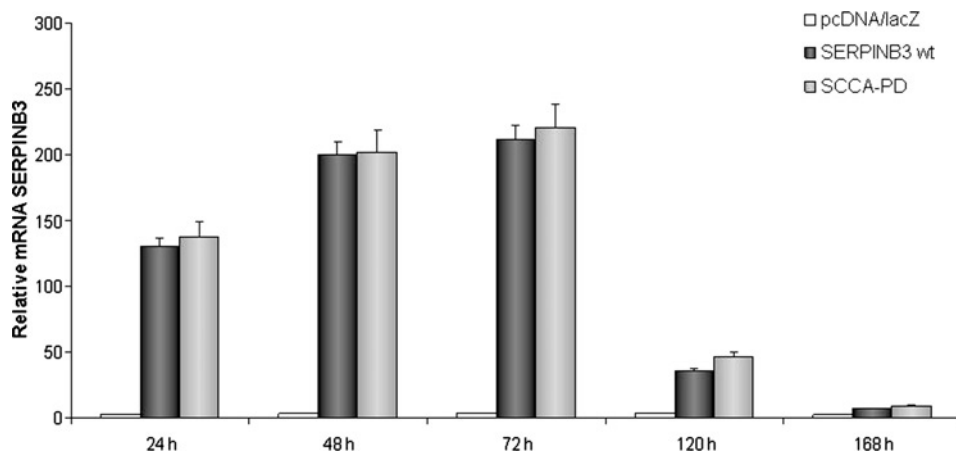


**Figure 1** Time course of SERPINB3 mRNA expression. HepG2 cells were transfected with wild-type SERPINB3 and SCCA-PD carrying vectors, while cells transfected with pcDNA3.1 empty vector were used as negative control. Data were normalized to GAPDH housekeeping gene and expressed as fold differences in mRNA SERPINB3 expression after normalization to the internal reference. The y-axis represents the relative mRNA level of the SERPINB3 gene calculated by  $2^{-\Delta\Delta C_T}$  method. Results are the average of three separate experiments performed in triplicate with the bars representing the standard error. GAPDH, glyceraldehyde 3-phosphate dehydrogenase

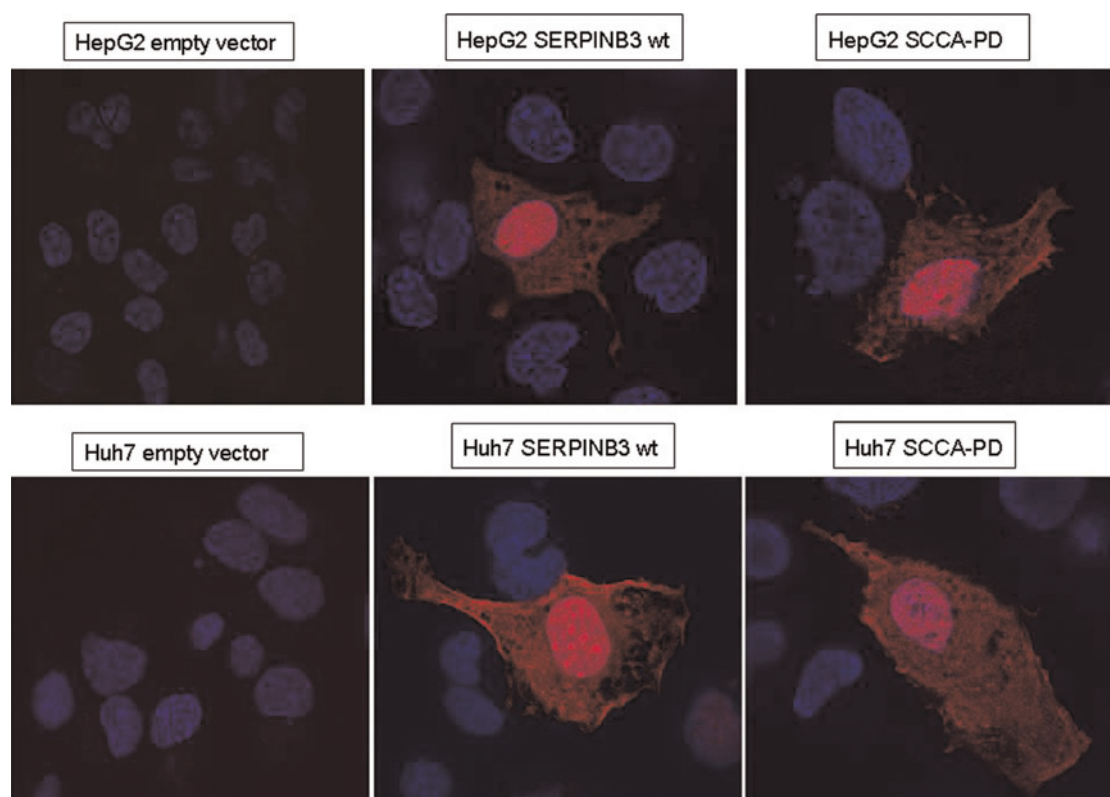


**Figure 2** Immunostaining for SERPINB3 in HepG2- and Huh7-transfected cells. Both cytoplasmic and nuclear protein expression are detectable in HepG2 and Huh7 cells transfected with the two SERPINB3 isoforms. WT, wild-type (A color version of this figure is available in the online journal)

between the two isoforms was detected: the second-order association constant was  $(3.5 \pm 0.7) \times 10^6 \text{ mol/L}^{-1}\text{s}^{-1}$  for SERPINB3 wild-type and  $(4.5 \pm 0.9) \times 10^6 \text{ mol/L}^{-1}\text{s}^{-1}$  for SCCA-PD. In this latter case the magnitudes of the association constants of the two SERPINB3 isoforms with cathepsin were similar, although SCCA-PD reacted faster than SERPINB3 wild type (Figure 5b).

### JNK1 kinase activity inhibition

The effect of SERPINB3 isoforms on the kinase activity of JNK1 was explored. As reported in Figure 6, densitometric

values showed that SERPINB3 isoforms inhibited the kinase activity of JNK1 in a dose-dependent manner. At high concentration (200 ng), SCCA-PD revealed a 16% higher inhibitory activity on JNK1-induced c-Jun phosphorylation, compared with SERPINB3 wild type.

### Molecular modelling of SERPINB3

Three-dimensional models of the wild-type SERPINB3 and its G351A polymorphic variant SCCA-PD were prepared by refining the crystal structure of the SERPINB3<sup>16</sup> followed by site-directed virtual mutagenesis G<sub>351</sub> → A (Figures 7a and b). To explore whether the G351A mutation in the putative P4 site of the variable reactive center loop may significantly change the conformational flexibility of the RSL, a short MD simulation on both SERPINB3 isoforms was carried out and the  $\varphi$  and  $\psi$  backbone torsion angles of the residue 351 was followed (Figures 7c and d).

The small difference in the  $\varphi$  and  $\psi$  backbone torsion angles of Gly351 in SERPINB3 and of Ala351 in the SCCA-PD isoform indicated that no significant conformational change in the RSL loop was expected to occur, due to the residue Gly351 replacement by the only slightly bulkier and more hydrophobic Ala residue.

### Discussion

A novel variant of the ov-serpin SERPINB3 (SCCA-PD) has been found by direct mRNA sequencing in liver tumors, presenting the 351<sub>G→A</sub> mutation in the reactive center of the

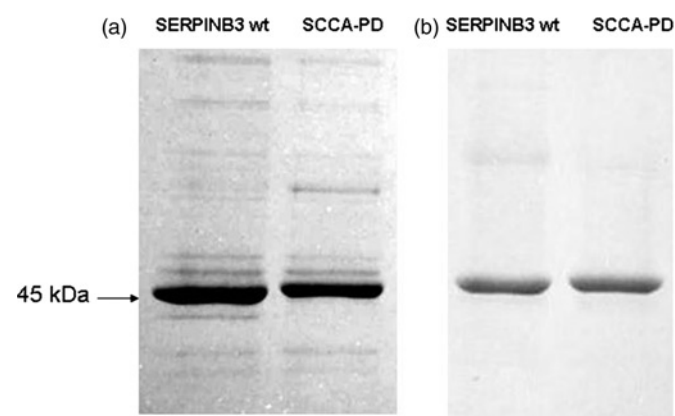


**Figure 3** SDS-PAGE/Coomassie staining. Recombinant SERPINB3 isoforms before (a) and after (b) ionic exchange chromatography purification. SDS-PAGE, sodium dodecyl sulfate polyacrylamide gel electrophoresis

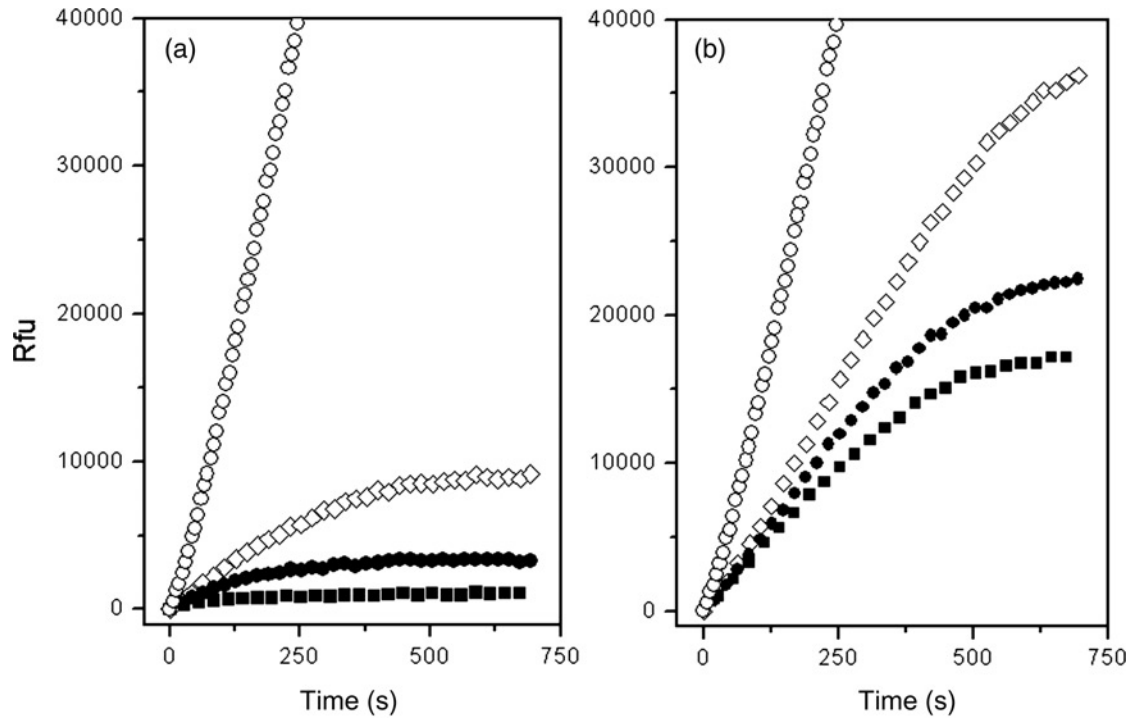


**Figure 4** Inhibition of papain by SERPINB3 isoforms. The interaction of papain with SERPINB3 wild-type and SCCA-PD was studied under pseudo-first-order conditions. In the study the substrate concentration was set to 500 nmol/L, while the concentration of enzyme was 1.5 nmol/L. The inhibitory activity of SCCA-PD (panel a) and wild-type SERPINB3 (panel b) was monitored by mixing different amounts of recombinant proteins (range concentration 0–100 nmol/L) with the substrate, and initiating the reaction by addition of the enzyme. The fluorescent product formation was monitored every seven seconds at 521 nm; for the sake of clarity, only a reduced number of data points are displayed. 0 nmol/L (○); 20 nmol/L (◇); 30 nmol/L (●); 50 nmol/L (■)

protein.<sup>3</sup> Previous studies indicate that the prevalence of SCCA-PD was 24% in the normal population and in patients with chronic hepatitis, while in patients with cirrhosis it was 45% ( $P = 0.038$ ),<sup>19</sup> supporting the hypothesis of a higher contribution of this isoform to liver disease progression. Recent

results indicate that SERPINB3 can induce RSL-dependent TGF- $\beta$ 1 synthesis and the effect is modulated by single amino acid mutation in the reactive loop.<sup>20</sup> In chronically damaged livers, a parallel over-expression of SERPINB3 and TGF- $\beta$ 1 was correlated directly to the fibrosis stage, as

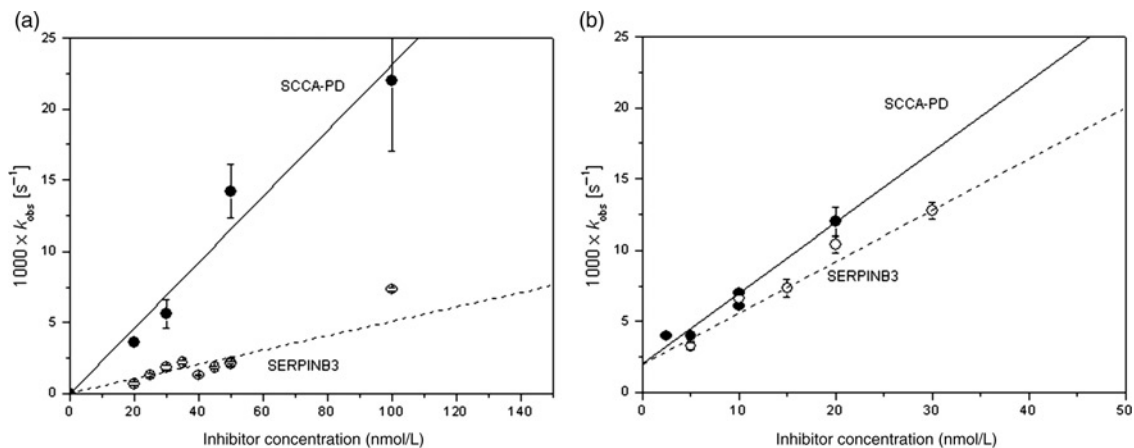


**Figure 5** Kinetics of the interaction between SERPINB3 isoforms and the cysteine proteinases papain and cathepsin-L. The dependence of the first-order constant on the concentration of the different SERPINB3 isoforms was determined from the data obtained by a non-linear fitting of the progress curves. The slope of the line interpolating the  $k_{obs}$  obtained at different concentrations of inhibitors represents the uncorrected second-order rate constant for the interaction between SERPINB3 isoforms and papain (panel a) and cathepsin-L (panel b). For each  $k_{obs}$  value reported in the graph, the error bars represent two times the uncertainty calculated by the fitting routine (wild-type SERPINB3/papain  $R = 0.95$ ,  $P < 0.05$ ; SCCA-PD/papain  $R = 0.95$ ,  $P < 0.05$ ). By correcting for the observed Michaelis–Menten constant of (ZFR)<sub>2</sub>R110 (650 nmol/L), the second-order rate constant for the association of SCCA-1 wild-type and SCCA-PD with papain resulted  $6.3 \times 10^4 \text{ mol/L}^{-1} \text{ s}^{-1}$  and  $4.1 \times 10^5 \text{ mol/L}^{-1} \text{ s}^{-1}$ , respectively. In the case of cathepsin-L, the error bars represent two times the uncertainty calculated by the fitting routine (wild-type SERPINB3/cathepsin-L  $R = 0.98$ ,  $P < 0.05$ ; SCCA-PD/cathepsin-L  $R = 0.95$ ,  $P < 0.05$ ). By correcting for the observed Michaelis–Menten constant of (ZFR)<sub>2</sub>R110 (27 nmol/L), the second-order rate constant for the association of wild-type SERPINB3 and SCCA-PD with cathepsin-L resulted  $3.5 \times 10^6 \text{ mol/L}^{-1} \text{ s}^{-1}$  and  $4.5 \times 10^6 \text{ mol/L}^{-1} \text{ s}^{-1}$ , respectively. Wild-type SERPINB3 (○); SCCA-PD (●)



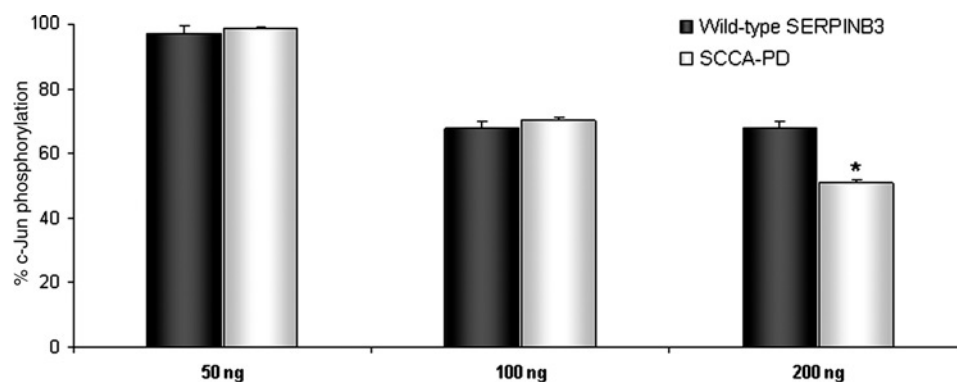


**Figure 6** Effect of SERPINB3 isoforms on the kinase activity of JNK1. Different concentrations of recombinant wild-type SERPINB3 or SCCA-PD protein were used to assess their effect on JNK1 activity, measured as c-Jun phosphorylation ability (SAPK/JNK kinase assay kit, Cell Signaling Technology). Results were derived by densitometric analysis of Western blot bands and were expressed as percent c-Jun phosphorylation, compared with controls (PBS). Bars represent mean  $\pm$  SD values of three different experiments. \* $P < 0.05$ : wild-type SERPINB3 versus SCCA-PD

a result of a dynamic interplay of these molecules, leading to progressive collagen deposition.<sup>20</sup>

Different mutations of the active loop have been described, altering the functional activity of SERPINB3.<sup>9,11</sup> However, no information is available for the SCCA-PD mutant. This study describes for the first time the increased inhibitory activity of SCCA-PD, compared with wild-type SERPINB3.

Among serpins, the hinge region in the RSL is well conserved.<sup>21</sup> In contrast, the amino acid sequences of the

variable portions resemble substrates in that they are complementary to the subsite specificities of the target proteinases. Previous studies have demonstrated that mutations within the hinge region (P15-P9) affected RSL mobility and the rate at which the RSL inserts into the body of the serpin. Mutation of the P14 residue to charged residues with large side chains blocked RSL insertion and abrogated the inhibitory activity, while mutation of P14 to uncharged residues had little effect.<sup>9,22–24</sup> In the present study,

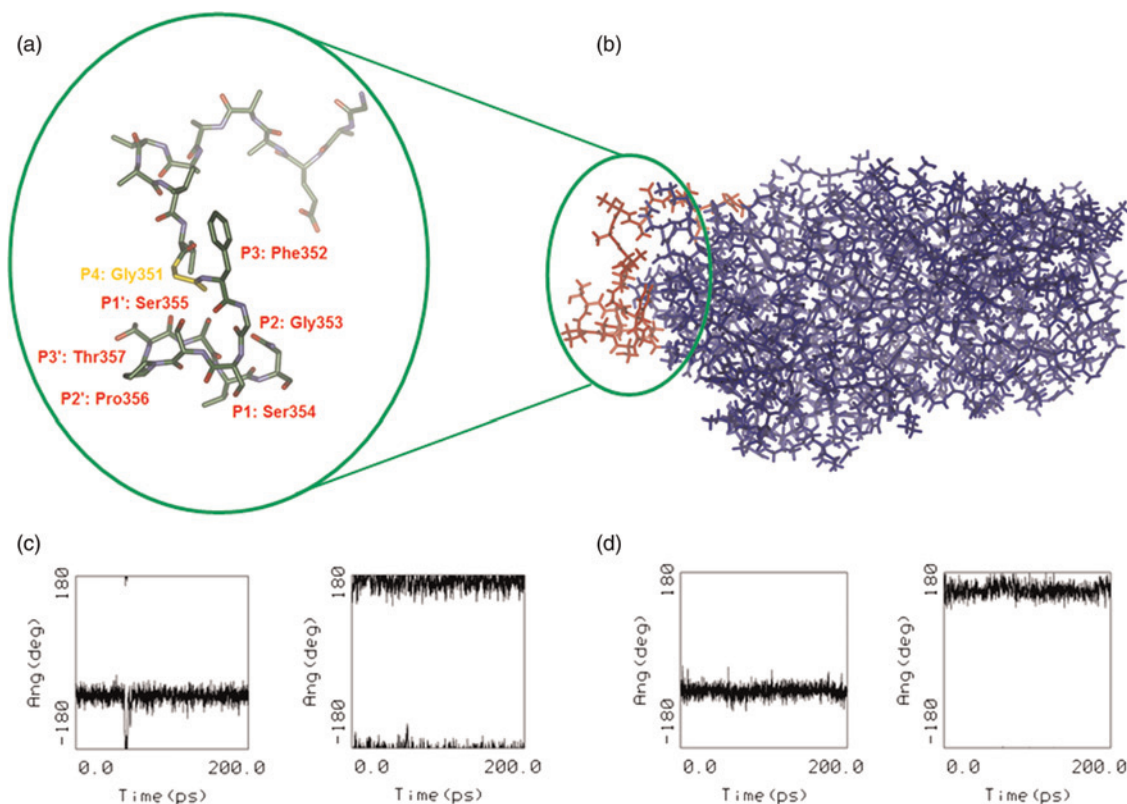


**Figure 7** Molecular modelling of SERPINB3. (a) Crystal structure of SERPINB3 with a detailed view of the RSL. Magnified reactive site loop (RSL) shows stick representation colored by atom type with the papain cysteine protease cleavage site recognition pattern labelled in the Schechter and Berger numbering scheme.<sup>38</sup> Hydrogen atoms are omitted for better clarity. Gly351 is shown in yellow color. (b) 3D molecular model of SERPINB3 obtained by molecular mechanics refinement of the crystal structure.<sup>16</sup> Position of the solvent exposed RSL is highlighted in red color. (c) Evolution of  $\phi$  and  $\psi$  dihedral angles of residues Gly351 and Ala351. Backbone dihedral angles of Gly351 residue fluctuate around average values of  $\phi = -60$  deg and  $\psi = 180$  deg in the wild-type SERPINB3 and (d) of mutated Ala351 in SCCA-PD isoform fluctuate around  $\phi = -60$  deg and  $\psi = 165$  deg during a 200 ps molecular dynamics simulation (A color version of this figure is available in the online journal)



**Table 2** Papain and cathepsin-L cleavage site preferences aligned with the sequence of RSL of SERPINB3 and SCCA-PD using the Schechter and Berger numbering scheme<sup>38</sup>

Papain Substrate	RSL variable region								
	S5 P5	S4 P4	S3 P3	S2 P2	S1 P1	S1' P1'	S2' P2'	S3' P3'	S4' P4'
Papain	X	HfoPoAr <sup>4</sup>	ArHfo <sup>3</sup>	ArHfo <sup>2</sup>	Arg <sup>1</sup> Lys	HfoArPo <sup>5</sup>	ArHfo <sup>6</sup>	ArPo <sup>7</sup>	X
Cathepsin-L	X	ArHfoPo <sup>11</sup>	ArPo <sup>10</sup>	ArHfoBs <sup>9</sup>	Arg <sup>8</sup> Lys	BsPo <sup>12</sup>	Ar <sup>13</sup>	Xp <sup>14</sup>	X
SERPINB3	V	G	F	G	S	S	P	T	S
SCCA-PD	V	A	F	G	S	S	P	T	S

RSL, reactive site loop

Papain:

<sup>1</sup>P1 – basic residues (Arg, Lys)<sup>30</sup><sup>2</sup>P2 – large aromatic residues (Phe, Trp, Tyr) partly also hydrophobic residues (Ala, Leu, Ile, Val),<sup>30,33</sup> (ArHfo – property mentioned first in the acronym has the priority, i.e. larger  $k_{cat}/K_m$  values for aromatic than for hydrophobic residues in P2)<sup>3</sup>P3 – aromatic residues (Phe) and hydrophobic residues (Leu)<sup>33</sup><sup>4</sup>P4 – hydrophobic (Leu), polar/basic (His and Lys) and aromatic (Phe)<sup>33</sup><sup>5</sup>P1' – hydrophobic residues (Leu) but not Val; aromatic residues (Trp), polar (Ser)<sup>30</sup><sup>6</sup>P2' – aromatic residues (Trp, Tyr, Phe) and hydrophobic residues (Leu)<sup>33</sup><sup>7</sup>P3' – aromatic residues (Tyr, Trp) and polar (Asn)<sup>33</sup>

Cathepsin-L:

<sup>8</sup>P1 – basic (Arg, Lys), aromatic and hydrophobic residues<sup>30,33</sup><sup>9</sup>P2 – aromatic residues (Phe, Trp, Tyr) and hydrophobic residues (mainly Leu, Ile)<sup>30,33</sup><sup>10</sup>P3 – aromatic residues (Phe, Trp) and polar/basic residues (His, also Lys)<sup>33</sup><sup>11</sup>P4 – aromatic residues (Phe), hydrophobic residues (Leu) and polar/basic residues (His)<sup>33</sup><sup>12</sup>P1' – basic and polar residues<sup>30,33</sup><sup>13</sup>P2' – aromatic residues (Trp)<sup>33</sup><sup>14</sup>P3' – some preference for small residues (Ala, Ser)<sup>33</sup>

evidence has been provided that the mutation to the P4Gly to Ala residue of SERPINB3, found in the SCCA-PD isoform, improves the antiprotease activity of this serpin, but had no effect on transfection efficiency, transcriptional activity, protein expression and cellular localization compared with SERPINB3 wild-type.

Kinetic analysis showed that SCCA-PD isoform displays an increased antiprotease activity against the cysteine protease papain, accounting for a 6.5 times faster association compared with SERPINB3 wild type isoform. Provided that the actual cleavage site (P1 P1') of papain corresponds in the numbering scheme of the RSL to residues Ser354 – Ser355 (Table 2), we may connect the increased rate of association with the active site specificity of papain. The active site of this protease consists of seven subsites (S1–S4 and S1'–S3'). Specificity is controlled by the hydrophobic pocket of the S2 subsite. Papain exhibits specific substrate preferences primarily for bulky hydrophobic or aromatic residues at the S2.<sup>25</sup> Beyond the S2 subsite preferences, there is a lack of clearly defined residue selectivity within the active site, but in general higher preference is given to hydrophobic residues including the S4 subsite (Table 2).<sup>25–28</sup> Therefore, increased hydrophobic profile of the SCCA-PD introduced by the G351A mutation in the P4 position (hydropathy score Gly: –0.4, Ala: 1.8)<sup>29</sup> may thus explain the observed elevated rate of association of the more hydrophobic RSL of SCCA-PD to papain compared with the wild-type SERPINB3.

Moreover, cathepsin-L displays substrate specificity similar to that of papain: hydrophobic amino acids at the positions P3 and P2 are necessary, and a further apolar amino acid at P1 may be helpful for rapid hydrolysis.<sup>30</sup> Little structural information is available from X-ray crystallographic studies on the S4 subsites of papain and cathepsin-L; it was uncertain whether these subsites

would participate in the binding.<sup>31–33</sup> However, some authors indicate that P4–S4 interaction exists because significant differences were observed in hydrolytic efficiency towards substrates with variations at the P4 position.<sup>33,34</sup> The S4 subsite of papain seems to exhibit specific substrate preferences primarily for bulky hydrophobic, followed by polar/basic and aromatic residues, while cathepsin-L shows preferences primarily for aromatic residues followed by hydrophobic and polar/basic residues (Table 2).

The analysis of cellular localization by immunofluorescence has demonstrated dual cytoplasm and nuclear localization for both isoforms in HepG2 and in Huh7 transfected cells, without any significant difference in distribution. Although it was initially reported that SERPINB3 is a cytosolic protein,<sup>35</sup> its nuclear localization has been also described recently, expanding the potential range of physiological functions of this molecule.<sup>36</sup> Nuclear translocation of SERPINB3 bound to c-Jun NH2-terminal kinase-1 (JNK1) after UV irradiation has been indeed described in keratinocyte cells,<sup>37</sup> resulting in inhibition of UV-induced apoptosis via the suppression of JNK1 activity. In the present study, we have confirmed that SERPINB3 suppresses JNK1 phosphorylation activity in a dose-dependent manner and we have provided evidence that SCCA-PD isoform has a better suppressive effect, at least at high protein concentration.

In conclusion, these results indicate that SERPINB3 polymorphic variants have different antiprotease activity and they might contribute differently to disease progression in injured tissue.

**Author contributions:** CT was involved in experimental design of the study and conducted realtime PCR, expression vector constructions, JNK assay and manuscript writing. AB and PPe performed kinetic analysis, VF performed

molecular modelling, SQ and MR performed immunofluorescence analysis and were involved in cell cultures. JZ and LB were involved in purification of recombinant proteins. SF, AG and GF were involved in the discussion of the results and in the reviewing of the manuscript. PPo was involved in the experimental design of the study, in the interpretation of the data and manuscript editing. All the authors declare that they have no competing interests.

## ACKNOWLEDGEMENTS

This work was supported in part by a grant from the National Ministry of Education, University and Research (FIRB Project Prot. RBLA03S4SP\_005) and by a research grant from the Associazione Italiana per la Ricerca sul Cancro (AIRC).

## REFERENCES

- Kato H, Torigoe T. Radioimmunoassay for tumor antigen of human cervical squamous cell carcinoma. *Cancer* 1997;**40**:1621–8
- Cataltepe S, Gornstein ER, Schick C, Kamachi Y, Chatson K, Fries J, Silverman GA, Upton MP. Coexpression of the squamous cell carcinoma antigens 1 and 2 in normal adult human tissue and squamous cell carcinomas. *J Histochem Cytochem* 2000;**48**:113–22
- Pontisso P, Calabrese F, Benvegnù L, Lise M, Belluco C, Ruvoletto MG, Marino M, Valente M, Nitti D, Gatta A, Fassina G. Overexpression of squamous cell carcinoma antigen variants in hepatocellular carcinoma. *Br J Cancer* 2004;**90**:833–7
- Giannelli G, Marinossi F, Trerotoli P, Volpe A, Quaranta M, Dentico P, Antonaci S. SCCA antigen combined with alpha-fetoprotein as serologic markers of HCC. *Int J Cancer* 2005;**117**:506–69
- Guido M, Roskams T, Pontisso P, Fassan M, Thung SN, Giacomelli L, Sergio A, Farinati F, Cillo U, Rugge M. Squamous cell carcinoma antigen in human liver carcinogenesis. *J Clin Pathol* 2008;**61**:445–7
- Worrall DM, Blacque OE, Barnes RC. The expanding superfamily of serpins: searching for the real targets. *Biochem Soc Trans* 1999;**27**:746–50
- Wells MJ, Sheffield WP, Blajchman MA. The clearance of thrombin-antithrombin and related serpin-enzyme complexes from the circulation: role of various hepatocyte receptors. *Thromb Haemost* 1999;**81**:325–37
- Luke C, Schick C, Tsu C, Whistock JC, Irving JA, Brömme D, Juliano L, Shi GP, Chapman HA, Silverman GA. Simple modifications of the serpin reactive site loop convert SCCA2 into a cysteine proteinase inhibitor: a critical role for the P3' proline in facilitating RSL cleavage. *Biochemistry* 2000;**39**:7081–91
- Schick C, Brömme D, Bartuski AJ, Uemura Y, Schechter NM, Silverman GA. The reactive site loop of the serpin SCCA1 is essential for cysteine proteinase inhibition. *Proc Natl Acad Sci USA* 1998;**95**:13465–70
- Perani P, Zeggai S, Torriglia A, Courtois Y. Mutations on the hinge region of leukocyte elastase inhibitor determine the loss of inhibitory function. *Biochem Biophys Res Commun* 2000;**274**:841–4
- Moore PL, Ong S, Harrison TJ. Squamous cell carcinoma antigen 1-mediated binding of hepatitis B virus to hepatocytes does not involve the hepatic serpin clearance system. *J Biol Chem* 2003;**278**:46709–17
- De Falco S, Ruvoletto MG, Verdoliva A, Ruvo M, Raucci A, Marino M, Senatore S, Cassani G, Alberti A, Pontisso P, Fassina G. Cloning and expression of a novel hepatitis B virus-binding protein from HepG2 cells. *J Biol Chem* 2001;**276**:36613–23
- Barrett AJ, Kembhavi AA, Brown MA, Kirschke H, Knight CG, Tamai M, Hanada K. L-trans-Epoxy succinyl-leucylamide(4-guanidino)butane (E-64) and its analogues as inhibitors of cysteine proteinases including cathepsins B, H and L. *Biochem J* 1982;**201**:189–98
- Schick C, Pemberton PA, Shi GP, Kamachi Y, Cataltepe S, Bartuski AJ, Gornstein ER, Brömme D, Chapman HA, Silverman GA. Cross-class inhibition of the cysteine proteinases cathepsins K, L, and S by the serpin squamous cell carcinoma antigen 1: a kinetic analysis. *Biochemistry* 1998;**37**:5258–66
- Schick C, Kamachi Y, Bartuski AJ, Cataltepe S, Schechter NM, Pemberton PA, Silverman GA. Squamous cell carcinoma antigen 2 is a novel serpin that inhibits the chymotrypsin-like proteinases cathepsin G and mast cell chymase. *J Biol Chem* 1997;**272**:1849–55
- Zhen B, Matura Y, Kumara T, Katagiri C, Hibino T, Sugiyama M. Crystal structure of SCCA1 and insight about the interaction with JNK1. *Biochem Biophys Res Commun* 2009;**380**:143–7
- Maple JR, Hwang MJ, Stockfish TP, Dinur U, Waldman M, Ewing CS, Hagler AT. Derivation of class II force fields. I. Methodology and quantum force field for the alkyl functional group and alkane molecules. *J Comput Chem* 1994;**15**:162–82
- Insight-II and Discover. Life Sciences software. Version 2005. San Diego, CA: Accelrys
- Turato C, Ruvoletto MG, Biasiolo A, Quarta S, Tono N, Bernardinello E, Beneduce L, Fassina G, Cavalletto L, Chemello L, Merkel C, Gatta A, Pontisso P. Squamous cell carcinoma antigen-1 (SERPINB3) polymorphisms in chronic liver disease. *Digest Liver Dis* 2009;**41**:212–6
- Turato C, Calabrese F, Biasiolo A, Quarta S, Ruvoletto M, Tono N, Paccagnella D, Fassina G, Merkel C, Harrison TJ, Gatta A, Pontisso P. SERPINB3 modulates TGF-beta expression in chronic liver disease. *Lab Invest* 2010;**90**:1016–23
- Gettins PGW. Serpins structure mechanism and function. *Chem Rev* 2002;**102**:4751–803
- Crowther DC, Evans DL, Carrell RW. Serpins: implications of a mobile reactive centre. *Curr Opin Biotechnol* 1992;**4**:399–407
- Huntington JA, Fan B, Karlsson KE, Deinum J, Lawrence DA, Gettins PG. Serpin conformational change in ovalbumin. Enhanced reactive center loop insertion through hinge region mutations. *Biochemistry* 1997;**36**:5432–40
- Lawrence DA, Olson ST, Palaniappan S, Ginsburg D. Serpin reactive center loop mobility is required for inhibitor function but not for enzyme recognition. *J Biol Chem* 1994;**269**:27657–62
- Worthington Enzyme Manual. *Enzymes and Related Biochemicals*. Freehold, NJ: Worthington Biochemical Corporation, 1993
- Kimmel J, Smith E. Crystalline papain. I. Preparation, specificity and activation. *J Biol Chem* 1954;**207**:515–8
- Alecio MR, Dann ML, Lowe G. The specificity of the S1' subsite of papain. *Biochem J* 1974;**141**:495–501
- Sigma-Aldrich Product Catalogue, Biochemicals and Reagents. St Louis, MO: Sigma-Aldrich, Inc, 2010
- Kyte J, Doolittle R. A simple method for displaying the hydropathic character of a protein. *J Mol Biol* 1982;**157**:105–32
- Kirschke H, Barrett AJ. Chemistry of lysosomal proteases. In: Glaumann H, Ballard FJ. *Lysosomes: Their Role in Protein Breakdown*. London: Academic Press, 1987:193–238
- Jia Z, Hasnain S, Hirana T, Lee X, Mort JS, To R, Huber CP. Crystal structures of recombinant rat cathepsin B and a cathepsin B-inhibitor complex. Implications for structure-based inhibitor design. *J Biol Chem* 1995;**270**:5527–33
- Turk D, Podobnik M, Kuhelj R, Dolinar M, Turk V. Crystal structures of human procathepsin B at 3.2 and 3.3 Å resolution reveal an interaction motif between a papain-like cysteine protease and its propeptide. *FEBS Letter* 1996;**384**:211–4
- Portaro FCV, Santos ABF, Cezari MHS, Juliano MA, Juliano L, Carmona E. Probing the specificity of cysteine proteinases at subsites remote from the active site: analysis of P4, P3, P2' and P3' variations in extended substrates. *Biochem J* 2000;**347**:123–9
- Taralp A, Kaplan H, Sytwu I, Vlattas I, Bohacek R, Knap AK, Hirana T, Huber CP, Hasnain S. Characterization of the S3 subsite specificity of cathepsin B. *J Biol Chem* 1995;**270**:18036–43
- Uemura Y, Pak SC, Luke C, Cataltepe S, Tsu C, Schick C, Kamachi Y, Pomeroy SL, Perlmutter DH, Silverman GA. Circulating serpin tumor markers SCCA1 and SCCA2 are not actively secreted but reside in the cytosol of squamous carcinoma cells. *Int J Cancer* 2000;**89**:368–77
- Izuhara K, Ohta S, Kanaji S, Shiraishi H, Arima K. Recent progress in understanding the diversity of the human ov-serpin/clade B serpin family. *Cell Mol Life Sci* 2008;**65**:2541–53
- Katagiri C, Nakanishi J, Kadoya K, Hibino T. Serpin squamous cell carcinoma antigen inhibits UV-induced apoptosis via suppression of c-JUN NH2-terminal kinase. *J Cell Biol* 2006;**172**:983–90
- Schechter I, Berger A. On the size of the active site in proteases. I. Papain. *Biochem Biophys Res Commun* 1967;**27**:157–62

(Received July 28, 2010, Accepted January 3, 2011)